INDIRECT STUDY OF NON-COVALENT PROTEIN COMPLEXES BY MALDI MASS SPECTROMETRY: ORIGINS, ADVANTAGES, AND APPLICATIONS OF THE "INTENSITY-FADING" APPROACH

Kevin M. Downard*
University of New South Wales, Sydney, NSW, Australia

Received 8 May 2015; revised 7 July 2015; accepted 7 July 2015

Published online 6 August 2015 in Wiley Online Library (wileyonlinelibrary.com). DOI 10.1002/mas.21480

This review article describes the origins, advantages, and application of an indirect approach with which to study protein and other macromolecular complexes and identify the nature and site of interaction interfaces by means of conventional matrix-assisted laser desorption ionization mass spectrometry (MALDI-MS). First reported in 1999, it involves the detection of ion depletion or the absence of ions associated with a binding partner or domain in the MALDI mass spectrum of a mixture of interacting components compared to that for an untreated control. Later referred to as intensity-fading in some applications, the method offers numerous advantages over the direct detection of protein and other macromolecule complexes by MALDI-MS and even electrospray ionization (ESI) MS. The origins of this indirect method, its development for use with gel-separated components, validation using companion biochemical assays, and application to a range of protein-antibody and protein–drug complexes are reviewed together with software specifically developed to aid with data interpretation. The sensitivity of the approach for revealing how subtle differences in the structure of the binding partners can be detected by MALDI-MS is also demonstrated. © 2015 Wiley Periodicals, Inc. Mass Spec Rev 35:559–573, 2016

Keywords: *non-covalent complexes; interactions; MALDI; indirect; intensity-fading*

I. INTRODUCTION

The direct analysis of protein and other macromolecular complexes by mass spectrometry began to be realized over 2 decades ago (Ganem, Li, & Henion, 1991a,b). It followed the development of electrospray ionization (ESI) just a few years earlier (Fenn et al., 1989). The ability of ESI to transfer large molecules, and subsequently their complexes, described by Fenn as "molecular elephants" (Fenn, 2003), directly from a solution environment into a mass spectrometer and detect them as charged ions, within instruments of limited dynamic mass range, proved to be revolutionary and worthy of a Nobel Prize (Fenn, 2003)

It was a few more years before peptide and protein complexes were also detected by means of matrix-assisted laser desorption ionization (MALDI) mass spectrometry (Rosinke et al., 1995; Tang et al., 1995; Woods et al., 1995; Cohen, Strupat, & Hillenkamp, 1997; Moniatte et al., 1997) including large protein complexes exceeding a mass of 150 kD (Kiselar & Downard, 2000). This proved to be a surprising development given the nature of the sample deposition and ablation processes.

Also considered a "soft" ionization technique by virtue of its ability to ionize large molecules without their fragmentation, MALDI-MS (Karas & Hillenkamp, 1988) offers advantages for such applications in terms of the ease with which samples can be prepared for analysis, the ability to overcome volatile solvent solubility constraints which limit ESI-MS, its greater tolerance to salts, buffers, denaturants, and other contaminants common in biological samples, the simple detection of complexes for the most part as singly charged ions rather than with a distribution of charge states (Downard & Kiselar, 2000), which lowers the signal intensity of each of them, and its suitability for high sample throughput by means of multi-target sample plates.

Although the desorption and ionization events during MALDI involve a range of optical phenomena, physicochemical and thermodynamic processes (Ehring, Karas, & Hillenkamp, 1992; Wang et al., 1993; Knochenmuss, 2002; Breuker et al., 2003; Dreisewerd, 2003; Karas & Krüger, 2003; Knochenmuss & Zenobi, 2003; Frankenvich et al., 2003), all of which are critical to ion formation and detection, the successful preservation of protein and other macromolecular complexes throughout sample deposition, the desorption and ionization events, extraction from the ion source, and flight through the mass analyzer to the ion detector have proven to be possible (Farmer & Caprioli, 1998; Bolbach, 2005; Downard, 2007).

Such direct analysis approaches, however, suffer from a number of challenges. First, given the typical low, often single, charge departed to molecules during the MALDI ionization process, large complexes must be detected on mass analyzers with a large mass range. The most suitable instrument in this regard use time-of-flight mass analyzers that, theoretically at least, have no upper mass limit (Madler et al., 2013). Yet, even with improvements to ion extraction (Colby, King, & Reilly, 1994; Brown & Lennon, 1995) and instrument design (Mamyrin, 2001; Satoh, Sato, & Tamura, 2007), these analyzers achieve relatively low mass resolution. Ions with high *m/z* values are, therefore, poorly resolved resulting in low mass accuracies. This problem is compounded by low detection sensitivities in the high mass range on most instruments so that ions of large protein complexes may go undetected.

An additional problem with the direct analysis of protein complexes by MALDI-MS is the inability to determine how the molecules in a complex are actually bound. The nature and site

Contract grant sponsor: Australian Research Council; Contract grant numbers: DP0449800, DP0770619, DP140100591.
**Correspondence to*: Professor Kevin Downard, University of New South Wales, Prince of Wales Clinical School, Sydney, NSW 2052, Australia. E-mail: kevin.downard@unsw.edu.au

of the interaction interface is not determined. Such information needs to be established in other experiments. Those that exploit mass spectrometry include hydrogen exchange (Konermann, Pan, & Liu, 2011), hydroxyl radical protein footprinting or radical probe mass spectrometry (RP-MS) (Maleknia & Downard, 2014), and chemical cross-linking (Mendoza & Vachet, 2009). However, these approaches all require that the interacting molecules are, in someway, labelled or modified.

II. ORIGINS OF THE INDIRECT MALDI-MS APPROACH; THE DETECTION OF PROTEIN–ANTIBODY INTERACTIONS AND LATER APPLICATIONS

To overcome these obstacles, without the need to chemically modify the interacting molecules, an indirect approach to detect macromolecular complexes using MALDI-MS was developed and first reported in 1999. This approach, initially applied to detect protein antigen–antibody interactions (Kiselar & Downard, 1999a) and assess the antigenicity of influenza virus strains at the molecular level (Kiselar & Downard, 1999b), provides a means with which to both detect macromolecular interactions and also identify the nature and site of the interaction interface.

Importantly, it also demonstrated for the first time that certain complexes could survive intact on a conventional MALDI surface while other non-binding components were ablated and ionized from it. Notably, this was achieved without any need to use preformed matrix surfaces (Law & Larkin, 2011), affinity-based (Hutchens & Yip, 1993; Tang, Tornatore, & Weinberger, 2004), or immobilization (Mock, Sutton, & Cottrell, 1992; Nelson et al., 1995; Nedelkov & Nelson, 2003) methods to bind one of the interacting partners to the MALDI plate or another insoluble surface such as a polymer bead.

The basis of the indirect approach, as described in the original article (Kiselar & Downard, 1999a), is illustrated schematically in Figure 1. A protein or other macromolecular complex is treated with protease and the mixture analyzed by MALDI-MS. Those regions of the binding partner(s) within the interface (shown in red) are not freely released into solution and thus their ions (highlighted in yellow) are depleted or absent in the spectrum of the complex versus that of an untreated control. Any other components present that do not interact, or which do not occupy the interface, are unaffected and appear with the same relative abundance in both spectra. The former can be removed where necessary with a pre-purification step.

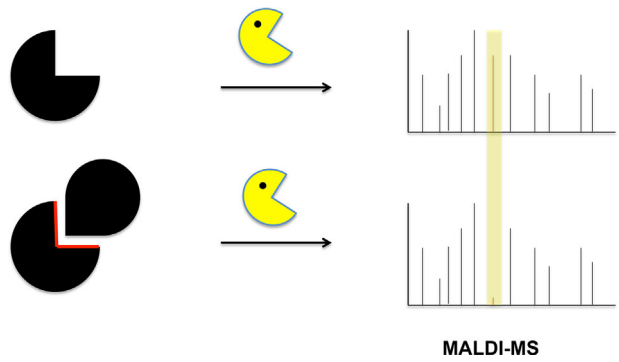

FIGURE 1. Schematically representation of the indirect MALDI-MS approach to identify protein or other macromolecular interactions.

Figure 2 shows the MALDI mass spectrum of an endoproteinase Glu-C digest of human lysozyme before and after its treatment with a monoclonal antibody. The upper spectrum (Fig. 2a) exhibits a range of peptide ions spanning the length of the protein with different intensities associated with their ionization efficiencies and other factors (Kratzer et al., 1998). The lower spectrum (Fig. 2b) is very similar in appearance except for the absence of peptide ions at *m/z* 1883. These correspond to residues 54–67 of the protein sequence. Peptide ions at *m/z* 4479 associated with a larger incompletely digested segment containing the same segment and comprising residues 54–91 are also found to decrease in relative intensity in the lower spectrum.

The relative areas of the ion peaks are compared in both spectra, relative to the base-peak or largest ion peak at *m/z* 1213, are shown in Table 1. Peak areas, rather than intensities, are preferred as these reflect the total ion current or population and compensate for the difference in mass resolution observed across a mass spectrum. Above an absolute difference of 10%, established as the experimental error based on replicate experiments across multiple studies, only the two segments identified above, and a third comprising residues 8–35, were found to decrease in relative area in the spectrum of the antibody-treated mixture. The formation and preservation of the antibody–peptide complexes on the MALDI sample plate throughout ion desorption and ionization provides indirect evidence for the presence of the complex while the proteolysis step enables the interacting residues to be identified.

In the same year as the initial study (Kiselar & Downard, 1999a), the detection of peptide–antibody complexes was reported from within a biological mixture of proteins (Kiselar & Downard, 1999b). The MALDI mass spectra following the tryptic digestion of a whole type A H1N1 influenza virus strain before and after treatment with a monoclonal antibody, that targets the surface hemagglutinin glycoprotein, is shown in Figure 3. Of the approximately 50 peptide ions detected in the spectra, the relative intensity of only one peptide ion at *m/z* 2210 differs across the two spectra by greater than 10% (absolute) with a relative difference of 56%. This peptide (highlighted) containing hemagglutinin residues 207–225 was found to bind the antibody. This region represents a highly accessible domain (shown in red) on the surface of the hemagglutinin trimer on the surface of the virus particle (Fig. 4).

The binding of this peptide segment to IgG antibody was independently corroborated by treatment of a synthetic mixture containing the epitopic peptide and two non-binding controls. Synthetic peptides comprising the C-terminal residues 214–225 were shown not to bind antibody, though the N-terminal portion of the larger peptide does. The ion signal for the peptide comprising residues 207–214 decreased in relative intensity by 64% after reaction with monoclonal IgG (Kiselar & Downard, 1999b). This region represents the refined epitope.

The success of the indirect MALDI method for the analysis of protein–antibody complexes with association constants typically of the order of $10^9 M^{-1}$ (Kiselar & Downard, 1999a,b) prompted others to apply the approach several years later. In these latter studies, the method was referred to as "intensity-fading" MALDI (abbreviated as IF-MALDI) (Villanueva et al., 2003). Although a convenient short-hand term, it is somewhat unfortunate in that relative peak area rather than intensity is a better measure of the population of analyte in a sample, as

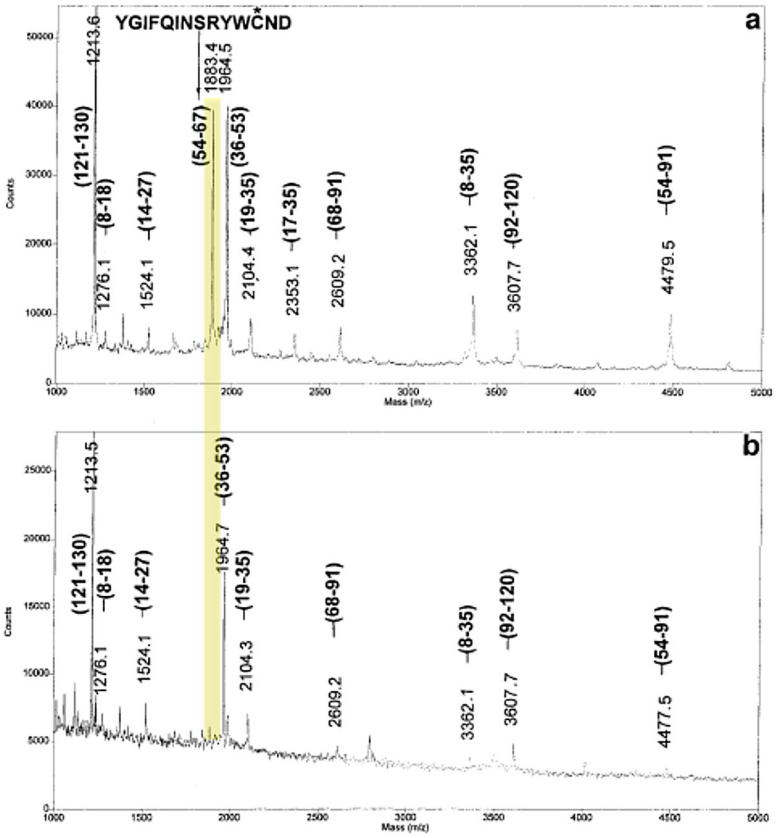

FIGURE 2. MALDI mass spectrum of the endoproteinase Glu-C digest products of human lysozyme (a) before and (b) after its treatment with a monoclonal antibody. Reprinted from Kiselar JG and Downard KM (1999a) with permission [American Chemical Society].

different peak widths associated with differences in mass resolution across a mass spectrum also impact on peak intensities. Thus, as the mass resolution decreases a peak will broaden and its intensity, quite apart from any other factors, will decrease. In contrast, the peak area is unchanged by mass resolution.

The authors of this latter study (Villanueva et al., 2003) applied the same approach described in the original work (Kiselar & Downard, 1999a), but without the proteolytic digestion to identify the binding peptides, to successfully detect both protease–inhibitor and protein–RNA interactions. A portion of solutions of typsin and carboxypeptidase inhibitors together with a non-binding protein were treated with protease and then analyzed by MALDI-MS against an untreated control. In the same study, the authors also reported the binding of one ribonuclease to RNA based on the decrease in its relative intensity compared with a non-binding control in the form of a procarboxypeptidase.

As no proteolytic digestion step was employed in this investigation, the presence of absence of complexes was established based solely upon the depletion of the parent ions for the inhibitor or ribonuclease in the mass range of 7,000–14,000. A marked decreased in the protease inhibitor signals were observed in the presence of protease attributed to the formation of protease–protease inhibitor complexes (Villanueva et al., 2003). In this study, potent protease inhibitors with low inhibitory constants (Ki) between 10^{-9} and 10^{-13} M were utilized. The inhibitory constant of a compound is the concentration at which it inhibits the protein's function by one half.

A cystatin–papain inhibitor–protease complex was also investigated by the same approach (Shabab et al., 2008). The selective decrease in the relative intensity of cystatin-treated papain was observed with respect to a non-binding control apomyoglobin added to the mixture. In this study, the concentration of cystatin was varied some 10-fold while the concentration of papain was fixed throughout. The concentration of free and bound cystatin was then determined based on the relative decrease in the ion intensity of free cystatin.

A more recent study by another group (Ma et al., 2013) investigated the application of the indirect approach to the study of calmodulin–alkaloid interactions with different MALDI matrices. Solutions containing each alkaloid, and the non-binding molecule propranolol, were added to an equimolar solution of calmodulin and then subjected to direct MALDI-MS analysis. When less acidic matrix solution preparations were used, the relative intensities of free alkaloid were significantly decreased after the addition of calmodulin compared to an untreated control spectrum. Competitive binding experiments were also performed in which equal quantities of two alkaloids were treated with calmodulin. This established a protein-binding affinity order (Ma et al., 2013) that was consistent with the results obtained by independent methods.

TABLE 1. Relative peak areas from MALDI mass spectra following endoproteinase Glu-C digestion of hen egg lysozyme without and with treatment with monoclonal IgG1 anti-lysozyme

residues	$[M + H]^+$ *m/z* (average)	relative peak area without treatment with IgG1 anti-lysozyme	relative peak area with treatment with IgG1 anti-lysozyme
121-130	1213.6	100	100
8-18	1276.1	4.6	6.0
14-27	1524.1	5.2	12.9
54-67	1883.4	79.3	0
36-53	1964.5	80.1	79.0
19-35	2104.4	15.8	13.9
17-35	2353.1	7.3	0
68-91	2609.2	13.0	10.6
8-35	3362.1	24.3	2.2
92-120	3607.7	22.4	12.4
54-91	4479.5	36.3	9.0

Although these additional protein–inhibitor (Villanueva et al., 2003; Shabab et al., 2008) and protein–alkaloid (Ma et al., 2013) studies were performed for a relatively small set of proteins on MALDI-TOF instruments with a large dynamic mass range, without the proteolytic digestion step required to establish the site of interaction, they nonetheless provided further evidentiary support for the preservation of specific protein complexes on the sample target key to the success of the indirect MALDI approach.

III. KEY CONDITIONS

In order to successfully implement these experiments, relative peak areas need to be compared from pairs of mass spectra. Although many factors influence the detection of ions by MALDI-MS, including the nature of the matrix, size, structure, and relative concentration of the compounds in the mixture, their relative areas should remain reasonably constant provided other experimental parameters used during the analysis of both samples remain constant.

A. Sample Deposition

One feature important to the successful application of the method is the need to reliably assess the relative levels of components within each sample in the form of their ions. For this reason, the deposition of the sample onto the target should be as uniform as possible, and ablation should take place from across the sample surface to produce spectra representative of the sample mixture. Both electrospray (Axelsson et al., 1997) and heat-assisted deposition, where the sample solution is more rapidly dried on the plate, can assist with the production of uniform, thin-layer sample surfaces so as to avoid local crystallization of analyte that gives rise to so-called "sweet spots," or areas in which more analyte is present and/or ion production is better over others.

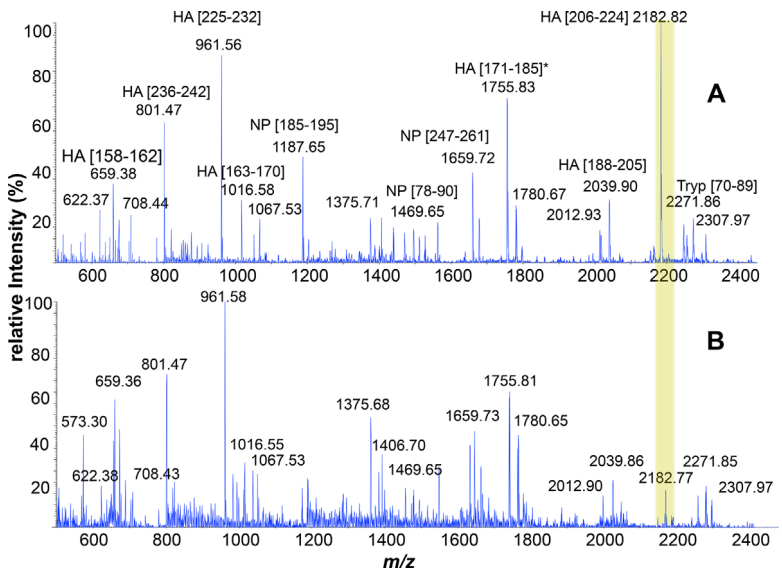

FIGURE 3. MALDI mass spectra following a whole virus tryptic digest of a type A H1N1 influenza strain (A) before and (B) after treatment with a monoclonal antibody that targets the hemagglutinin. Reprinted from Kiselar JG and Downard KM (1999b) with permission [American Chemical Society].

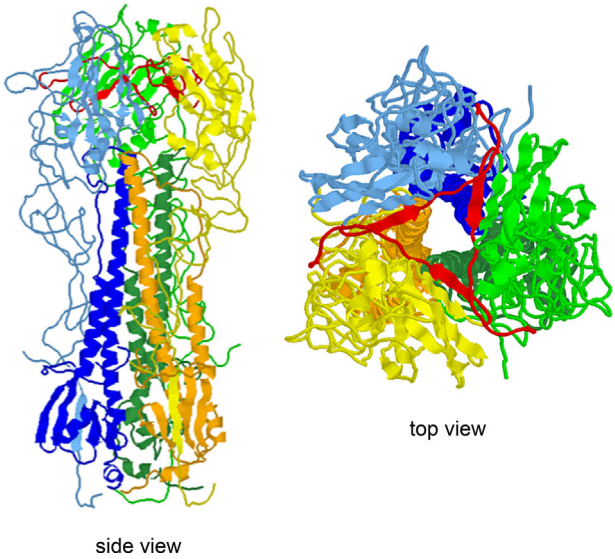

FIGURE 4. Side and top view of the influenza hemagglutinin trimer showing the HA1 (light blue, green, yellow) and HA2 (blue, dark green, orange) subunits together with the epitope (red) recognized by the monoclonal antibody as identified in Figure 3. Reprinted from Kiselar JG and Downard KM (1999b) with permission [American Chemical Society].

B. Laser Ablation

Provided the uniform deposition criterion described above is met, no reduced laser fluence or ablation time is required to achieve the indirect MALDI-MS approach. Sample can be ablated from the across surface using dozens of shots at laser powers typical of other experiments (Dreiseverd et al., 1995). Most modern MALDI-based instruments feature a so-called raster option in which sample is ablated from across the sample by the automated repositioning of the laser, or the target relative to the laser beam, by a distance that is less than the diameter of the laser beam. The acquisition software can further be programmed to store only those spectra where the signal-to-noise ratio exceeds a certain base threshold. In this manner, spectra can be acquired and summed from across the deposited sample with good spatial resolution.

C. Chemical Additives and Acidic Matrices

One condition that is key to the success of the method is the need to avoid, or at least reduce, the presence of solvents, denaturants, or other chemical agents that may dissociate the deposited complex prior to or during its deposition. The presence of additional acid, such as acetic or trifluoroacetic acid, in the matrix solution has been noted as problematic in this regard (Kiselar & Downard, 1999a). It was shown that the addition of a 1% trifluoroacetic acid solution to the matrix solution released the peptide from the bound complex with the IgG antibody. This led to their detection, rather than their depletion or absence, in the MALDI spectrum of the treated mixture. The same affect may be observed if organic solvents or other denaturants are present in the mixture.

In this regard, some compromise is reached between the need to employ acidic matrix compounds such as α-cyano-4-hydroxycinnamic acid to promote ionization, and organic solvents such as acetronitrile to dissolve them, and the desire to keep solutions free of these in order to preserve the integrity of a complex.

Results of the protein lysozyme study (Kiselar & Downard, 1999a), and for the influenza virus strain (Kiselar & Downard, 1999b), showed that the solution-specific associations between monoclonal antibodies and their target antigens can be preserved on the MALDI target after deposition in an α-cyano-4-hydroxycinnamic acid matrix solution at a pH∼3 (Fig. 4). When trifluoroacetic acid was added to the matrix solution, lowering the pH of the solution below a value of 2, dissociation of the antibody complexes occurred. This resulted in the subsequent increase in the relative area of the ions of binding peptides in the MALDI spectrum of the antibody-treated mixture such that the interaction could not be established (Kiselar & Downard, 1999a).

Similar conclusions were reached in the study of protease inhibitor complexes (Yanes et al., 2007). The investigation of the effects of different matrix solutions at different pH, with and without the use of thin layer deposition, on the stability of two protease inhibitor complexes, and thus the relative intensity of the ligand, was largely unaffected by pH in the range of 2.5–5.5 (Yanes et al., 2007) but could be disrupted below this pH range.

D. Relative Ratio of Interacting Partners

Subject to the affinity of the interacting partners (Erijman, Rosenthal, & Shifman, 2014), it may be necessary to adjust their relative concentration in solution in order to ensure that sufficient levels of complex are formed for detection purposes. The initial studies (Kiselar & Downard, 1999) employed approximately equimolar quantities of protein antigen and antibody due to the high specificity and affinity of antigen–antibody complexes with typical association constants of between 10^8 and $10^{11}M^{-1}$. Later drug binding studies, however, utilized an excess concentration of drug to protein of the order of 5:1 in order to ensure the protein–drug complexes were formed and detected (Nasser et al., 2013; Swaminathan & Downard, 2012; Swaminathan et al., 2013, 2014).

Increasing the concentration of one binding partner further can result in undesirable consequences. When protein concentrations were increased by a factor of 15–20 over that of an inhibitor, protein–protein complexes in addition to protein–inhibitor complexes were detected (Yanes et al., 2007). The use of high relative concentrations of one of the analytes can also result in the undesirable formation of non-specific complexes.

E. Choice of Enzyme/Protease

Where an interaction interface within a protein complex is under investigation, a protease is used to release peptides not located within that interface. Cleavage sites that are located within an interaction interface are at least partly shielded from the protease and thus their release is restricted compared to when the same protein is not in complex (Fontana et al., 2004).

In the case where some information about the location of the interaction interface is known, or surmised, a judicious choice of protease can be made. Where no such information is available, a process of trial and error is employed. Often two separate proteolysis experiments may be necessary in order to refine the interaction interface.

A highly site-specific protease such as trypsin is often the enzyme of first choice. Trypsin cleaves predictably and reliably at the C-terminal side of lysine and arginine residues producing peptides that typically also ionize well by virtue of their basic amino acid character. However, tryptic cleavage sites may not reside near the interaction interface necessitating that another endoprotease such as Glu-C, Lys-C, or Asp-N be used. Note that an enzymatic, over chemical, cleavage is preferred in order to ensure that physiological-like solution conditions are employed.

F. Initial Intensity and Sequence Coverage of Peptide Ions in Control Spectrum

Even with the appropriate choice of protease, ions detected within the mass spectra of protein digests rarely reflect all peptide segments. Proteases cleave along a protein backbone at different rates irrespective of the presence of a common residue at the cleavage site. Ionization and detection efficiencies (Shigeri et al., 2012), in addition to suppression effects (Kratzer et al., 1998), also contribute to this phenomenon. As such, of those peptide ions detected, some will have a lower intensity within the untreated sample, control spectrum. This limits the ability of the indirect method to follow their participation in the interaction interface. In this respect, an ion signal should have an area or intensity that exceeds at least 10% of the base, or most abundant, peak in order that its involvement in binding can be followed through the peak reduction approach. The use of two separate proteolysis experiments, as described above, can assist in this regard since a peptide segment absent or detected with low intensity following one proteolysis experiment, may appear more prominently in the control spectrum when a different endoprotease is used.

IV. INCORPORATION OF A GEL-BASED SEPARATION STEP

In order to extend the approach to larger biological mixtures as part of a proteomics strategy for analyzing protein interactions (Downard, 2006, 2013), the original studies (Kiselar & Downard, 1999a,b) were extended to gel-recovered proteins (Morrissey & Downard, 2006). The complete or partial purification of component proteins or protein complexes by gel electrophoresis offers the benefit of reducing the number of peptides detected by mass spectrometry. This reduction in the complexity of the spectrum results in improved peptide sequence coverage within the proteins of interest. This subsequently improves the possibility that binding peptides are detected in the control spectrum and a reduction in their peak area can be followed.

A recombinant hemagglutinin related to that detected in the study of the whole virus digest (Kiselar & Downard, 1999b) was first resolved in-gel ahead of its proteolytic digestion and treatment with a monoclonal antibody. In accord with results of an earlier study for a related type A H1N1 strain (Kiselar & Downard, 1999b), hemagglutinin residues 206–224, and to a lesser degree those that flank this region comprising residues 226–235 and 188–205, were found to bind the antibody in the case of both the Beijing and diverged New Caledonia strains. This determinant differs in the Beijing strain (Morrissey & Downard, 2006) only at position 223 where serine replaced asparagine. The relative area of the ions corresponding to peptide 206–224 were found to decrease by 94% (absolute) after incubation with the antibody compared to the untreated control.

Importantly, greater sequence coverage was afforded by the gel-separation step (Morrissey & Downard, 2006). The coverage within the spectrum of the trypsin-digested hemagglutinin represented 45% of the protein sequence, over twice that observed when the whole virus was digested (Kiselar & Downard, 1999b). This is despite the fact that resolution of the hemagglutinin on the gel was incomplete, such that peptides representing 38% of the viral nucleoprotein were also identified in the same spectrum (Morrissey & Downard, 2006). This greater sequence coverage considerably improves the probability that the binding peptide will be detected in the control spectrum, and a decrease in its relative ion signal can, therefore, be followed in the antibody-treated mixture.

An initial gel-purification approach was also successfully employed to identify antibody-binding regions within the viral hemagglutinin of three type A H3N2 influenza strains (Morrissey, Streamer, & Downard, 2007). Monoclonal antibodies raised to viruses of the H3N2 serotype were reacted with gel-recovered protein containing primarily the hemagglutinin antigen. Four antigenic domains of hemagglutinin were localized to residues 109–125, 158–170, 158–183, and 316–326 that, with the exception of residue 158, shared common sequences across all three strains. Two segments involving residues 19–125 and 316–326 represent determinants occupy exposed regions atop the HA1 subunit and likely form a non-continuous conformational epitope. The third across residues 158–183 is located on a stem region closer to the adjoining HA2 subunit. These binding sites have been previously identified as antibody binding domains in independent investigations.

Where it is desirable to purify the protein complex, rather than one of the binding components, native gel electrophoresis can be employed. To facilitate the recovery of protein complexes from a native gel prior their digestion, an optimal gel-recovery method was developed (Mackun & Downard, 2003). Gel plugs containing proteins excised from the gel were resuspended in a buffered solution and then sonicated within a bath sonicator with periodic cooling on ice. Protein recovery levels of between 70 and 80% were achieved by this approach that were superior to other tested approaches including passive diffusion or cell probe sonication methods (Mackun & Downard, 2003).

V. SOFTWARE TO AID DATA ANALYSIS

An algorithm has been developed to aid with the identification of the binding partners through a comparison of a pair of MALDI mass spectra (Ho et al., 2007). Known as PRISM, for PRotein Interactions from the Spectra of Masses, the algorithm features a graphical user interface in which to display and process the mass spectra. Lists of *m/z* values and peak areas or intensities extracted from raw datasets are imported in text file format. These are pre-processed to remove both ions of low signal-to-noise, relative to the most abundant base peak (default 1%), and those that do not share a common mass-to-charge ratio value in the control and reaction spectrum within a specified mass error (default 0.1%).

In order to compare changes in relative peak area across two different mass spectra, the algorithm initially establishes a so-called "constant peak." The constant peak is determined by measuring the ratio of the areas of all adjacent peaks (denoted n

and n+1) in the control sample spectrum. The peak (n) for which the absolute difference in relative area is the smallest is assigned to be the constant peak. The value for the relative area of the constant peak to the base peak within the control sample spectrum is then used to establish an "imaginary peak" in the spectrum of the reacted mixture so that the ratio of area of the constant peak to the imaginary peak is identical to this value.

The algorithm then compares the absolute difference in relative area across both spectra relative to the base peak and imaginary peak in the control and reaction mixture spectra, respectively. The data are output as a list of potential binding peptides above an assigned relative area difference (default 10%). The identity of the constant peak, its area, and that of the imaginary peak are also reported.

The MALDI mass spectra recorded following the binding of antibody to a partially gel-separated viral hemagglutinin (Morrissey & Downard, 2006) was input into the PRISM algorithm. The visualized output is shown in Figure 5. Scalable spectra are shown in the upper portion of the output while the computational summary containing the peptides whose relative peak areas decrease above the prescribed tolerance are shown in the lower field. Note that subject to spectral quality, the noise threshold and peak area tolerance (default 10%) can be adjusted and the spectra reanalyzed. Consistent with the manual interpretation of the data, the peptide segment comprising residues 206–224 which appear as ions at *m/z* 2181.8 are identified as those which bind to the antibody together with residues 188–205 (*m/z* 2038.9) that flank this site.

Although applied in this example to mass spectral data recorded to help identify protein interactions, the PRISM algorithm has broader utility for the comparison of any two mass spectra. It can prove be beneficial, for instance, in the identification of differences in mass spectra that derive from the different structural features of two closely related molecules (Ho et al., 2006).

VI. APPLICATION TO THE KINETICS OF PROTEIN ANTIGEN–ANTIBODY COMPLEXES

In addition to the applications described in Sections II and IV above, the indirect MALDI approach was further applied to study the kinetics of protein antigen–antibody interactions using a time-course approach. The implementation of a time-course experiment enables the relative rates at which epitopic peptides bind to antibodies to be assessed in both non-competitive and competitive immunoassays. Where peptides of closely related sequence are studied, the importance of specific amino acid residues to the interaction can be assessed.

A time course MALDI mass spectrometry immunoassay was employed (Morrissey & Downard, 2008) to study the relative rates of binding of two epitopic peptides comprising residues 109–125 and 158–166 derived from influenza hemagglutinin. The binding of the peptides was followed within the whole digest mixture after their incubation with antibody over a 0–24-hr period. Spectra were recorded and compared with an unreacted control.

Plots of the relative areas recorded for these peptide ions signals over the time course are shown in Figure 6. The relative area for HA peptide comprising residues 109–125 is seen to decrease from over 110% to some 40% over 24 hr while that for HA peptide 158–166 decreases from almost 50% to zero over the same period. The areas were best fit to a first order exponential decay function ($y = A.e^{-kx}$) where y represents the relative peak area, x is the incubation time, A is a

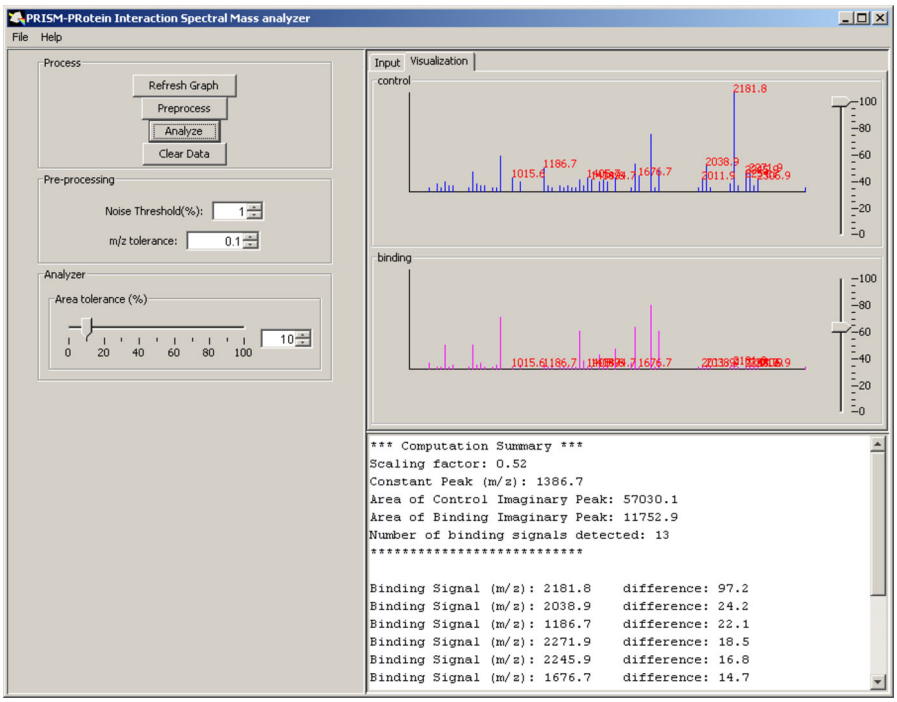

FIGURE 5. Graphical user interface of the PRISM algorithm showing the processing of the spectra of Figure 3. Reprinted from Ho JWK, Morrissey B, Downard KM. (2007) with permission [Springer].

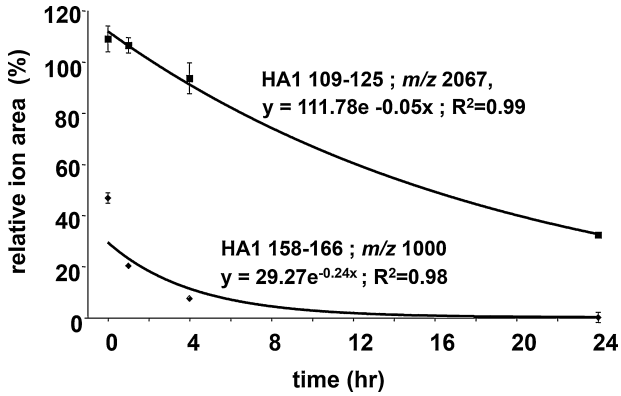

FIGURE 6. Plot of the relative peak area for the ions of two epitopic peptides following their treatment with a monoclonal antibody over a 24 hour period. Reprinted from Morrissey B, Downard KM. (2008) with permission [American Chemical Society].

constant and the coefficient k defines the rate of peptide binding. The binding rate for the two peptides was found to differ by a ratio of some 5 to 1.

A shorter peptide comprising HA residues 119–125 (of sequence PDYASLR) was also found to bind to antibody. The relative rate of binding of this peptide was subsequently compared to the larger epitope (residues 109–125) using the indirect MALDI-MS approach. It was shown to bind at twice the rate of the larger epitopic peptide suggesting that its smaller size minimizes steric constraints that impede binding.

To establish the effect of amino acid substitutions on the rate of binding, a series of eight peptides based on the sequence of the smaller epitopic peptide were synthesized. Non-competitive time course immunoassays were conducted for each of the eight peptides in the presence of two non-binding control peptides. This study found that four of the eight peptides bound to antibody while the other four did not. Only those in which substitutions were made in the C-terminal portion of the peptide at residues 123 (S to A) and 125 (R to E or L) were shown to still bind antibody. Furthermore, the rates of binding among the four binding peptides were largely unchanged by the substitutions. Their relative binding rates differed only by a factor of less than two and no preferential binding among the three substituted peptides was found in competitive binding experiments.

VII. COMPARISON OF THE MALDI-MS APPROACH WITH RESULTS OF HEMAGGLUTINATION INHIBITION (HI) ASSAYS

In order to demonstrate both the effectiveness and validity of the indirect MALDI-MS approach for identifying and screening the antigenicity of influenza virus strains (Downard & Morrissey, 2007), the results of the method were compared side-by-side with those obtained from conventional hemagglutination inhibition assays (Schwahn & Downard, 2009).

The hemagglutination inhibition assay is a widely used, non-molecular-based approach to assess whether antibodies produced within blood sera following infection, cross react with other circulating influenza strains (Katz, Hancock, & Xu, 2011). The attachment of the influenza virus to red blood cells (RBCs) results in agglutination that impedes their sedimentation within a titer plate. Hemagglutination is inhibited if sufficient quantities of antibodies present are bound to hemagglutinin that in turn prevents the virus from attaching itself to the RBCs. The inhibition of hemagglutination by antisera or monoclonal antibodies is utilized in the assay to determine the serotype of viral strains.

Although this serological assay forms the basis of present day screening of the virus, it is not without its limitations. For example, non-specific hemagglutination inhibitors in sera can lead to false positive results unless removed or destroyed. Further problems can result from the variations in strains to hemagglutinate RBCs of different animal species. In addition to these practical considerations, the HI assay provides no molecular detail or information about the structural changes that underlie antigenic drift or shift.

A side-by-side comparison of the MS and HI assays was undertaken in a study of the binding of antibodies that separately target type A and type B influenza strains. The MALDI mass spectra of the tryptic peptides from a partially resolved mixture containing both influenza hemagglutinin and nucleoprotein of a type A H1N1 strain with no antibody and after incubation with either mAb154 (anti-influenza type B) or mAb128 (anti-influenza type A) are shown in Figure 7.

No appreciable differences in the ions detected, nor their relative areas, were apparent between in the spectrum of the digested viral proteins of the type A H1N1 A/New Caledonia/20/99 strain without antibody or that treated with influenza B-specific antibody mAb154 (Fig. 7A and B). In contrast,

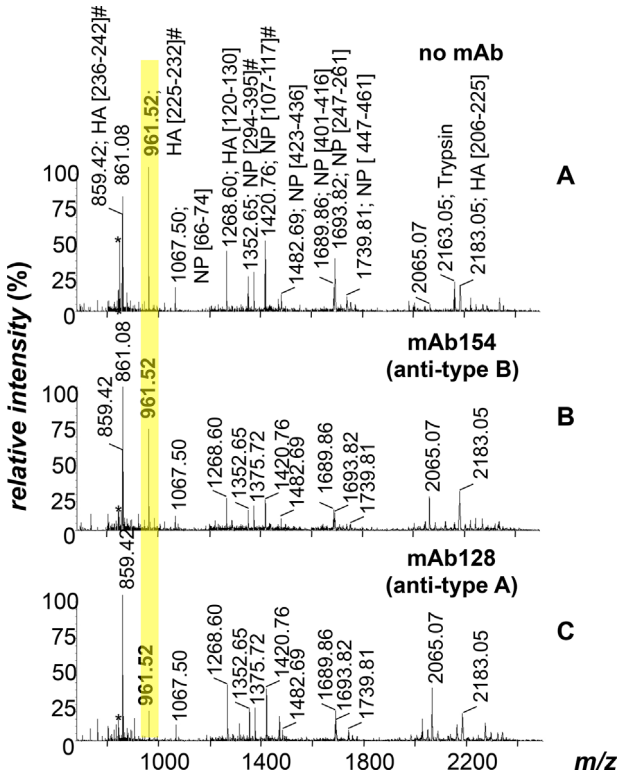

FIGURE 7. MALDI mass spectra of the tryptic digest products of a partially resolved mixture containing influenza hemagglutinin and nucleoprotein of a type A H1N1 strain with (A) no antibody, (B) following incubation an anti-influenza type B antibody, and (C) following incubation an anti-influenza type A antibody. Reprinted from Morrissey B, Downard KM. (2008) with permission [Wiley].

treatment of the peptide mixture with monoclonal antibody mAb128 to type A influenza results in a significant decrease in the relative area of the peptide ions at *m/z* 961.5 (Fig. 7C, highlighted) corresponding to HA residues 225–232. In accord, the mAb128 antibody inhibited hemagglutination against the type A virus down to concentrations of 2 ng/μL. It failed to do so at all concentrations up to 125 ng/μL against the type B Tokyo/53/99 virus. In contrast, the mAb154 antibody to type B viruses of the Yamagata lineage down to 0.4 ng/μL but not the type A strain. Thus immunodominant epitopes within the hemagglutinin antigen can be identified by the MALDI-MS approach and the results are largely in accord with the HI assays.

VIII. APPLICATION TO PROTEIN–DRUG/INHIBITOR COMPLEXES

A. Inhibitors to Influenza Neuraminidase

Inhibitors to influenza neuraminidase (NA) are the most widely administered against the virus. They function by blocking the active sialic-acid-binding site of the enzyme to prevent it from detaching progeny virus particles from the host cells' sialic acid receptor. This inhibition of virus replication, late in the replication cycle, prevents the rise in viral progeny and thus reduces the symptoms and duration of illness. Zanamivir and oseltamivir are the neuraminidase inhibitors most often prescribed. They are based on a natural sialic acid inhibitor known as 2-deoxy-2,3-didehydro-N-acetylneuraminic acid or DANA.

The indirect MALDI approach correctly established the binding sites of zanamivir and DANA based on available X-ray crystal data (Swaminathan & Downard, 2012). Solutions of influenza neuraminidase were incubated with a fivefold excess of either DANA or zanamivir and compared with results for a non-binding control compound. To reduce the presence of contaminants in the spectra, the complexes were first passed through a native gel and recovered by so-called blind excision with gel-sonication as described earlier in Section IV (Mackun & Downard, 2003). Blind excision is employed to avoid the use of a visualization stain that may cause denaturation or dissociation of the complex. A single stained reference band is used to locate the position of the protein or complex (Fig. 8).

The gel-recovered neuraminidase–inhibitor complexes and untreated control were digested separately with either trypsin or endoproteinase Glu-C. Two tryptic peptide segments corresponding to NA residues 119–130 and 157–172 of the protein were shown to bind to both zanamivir and DANA but not a control compound based on an absolute decrease in their relative peak areas of 31.4 and 26.5%, and 26.0 and 18.5%, respectively (Swaminathan & Downard, 2012). Two different binding peptide segments were detected in the case of the spectra for the Glu-C digested mixtures. These peptides comprise NA residues 277–286 and 402–412 that were found to decrease in relative peak area by 23.7 and 16.7% for zanamivir and 10.6 and 13.3% for DANA. The combined data from both digests revealed all of the binding peptides contained residues known to reside within the active site; namely Arg118, Glu119, Arg156, Glu276, and Tyr406. The latter has been shown to be a key catalytic residue that may function as a nucleophile and which can covalently bind inhibitors (Vavricka et al., 2013).

Following this demonstration that the indirect MALDI-MS approach could reliably identify inhibitor/drug-binding sites, the method was applied to investigate the inhibitory potential of other compounds. This is of importance given the rise in the number of strains resistant to both oseltamivir and zanamivir.

One such compound is cyanidin-3-sambubiocide, an anthocyanin present in high concentration in berries and grapes (Fig. 9). The binding of the anthocyanin to influenza neuraminidase was investigated by the indirect MALDI-MS approach in conjunction with parallel computational molecular docking (Swaminathan & Downard, 2013). The MALDI mass spectra of the Lys-C/Glu-C peptides released from the untreated and anthocyanin treated neuraminidase are shown in Figure 10. Two neighboring peptides comprising NA residues 403–412 and 412–425 were found to bind to the anthocyanin based on decreases in their relative peak areas of 14.0 and 30.7% in replicate experiments.

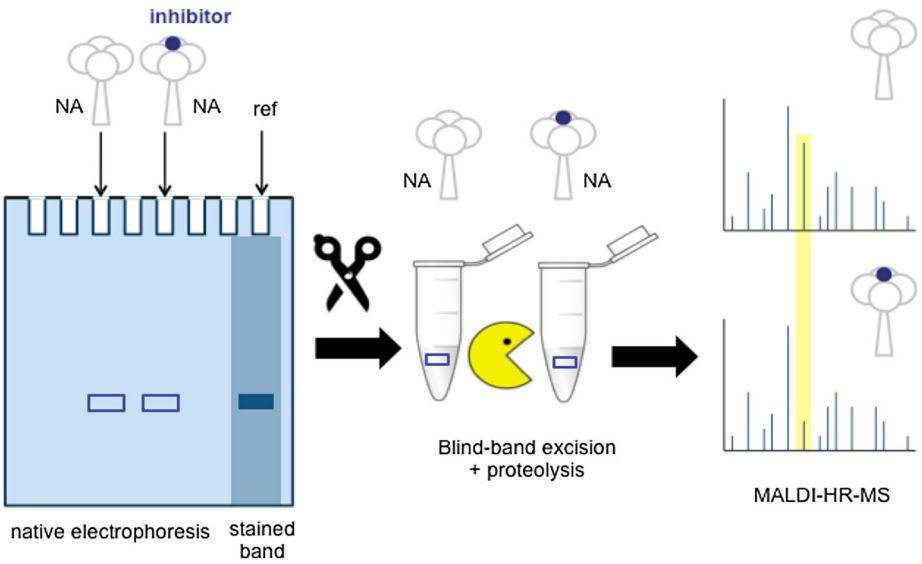

FIGURE 8. Schematic representation of the indirect MALDI approach incorporating a native gel separation step with blind band excision for the identification of protein-inhibitor complexes.

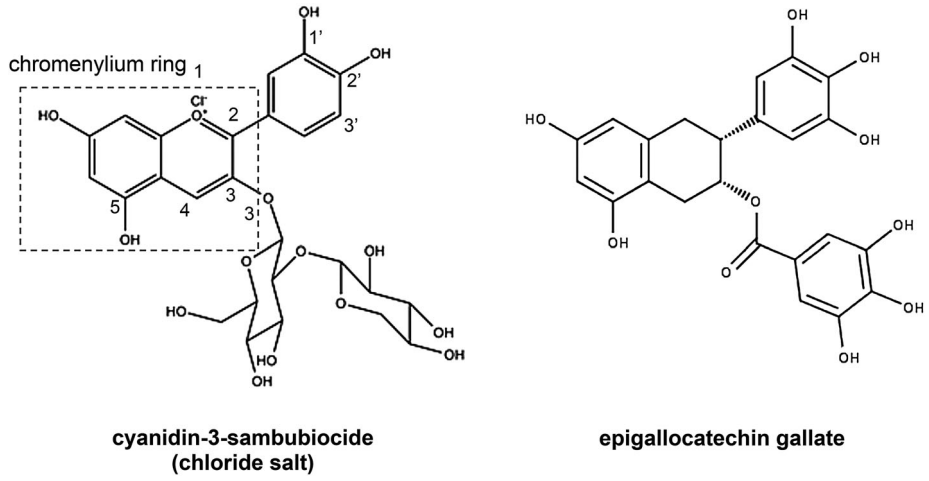

FIGURE 9. Chemical structures of cyanidin-3-sambubiocide (as a chloride salt) and epigallocatechin gallate.

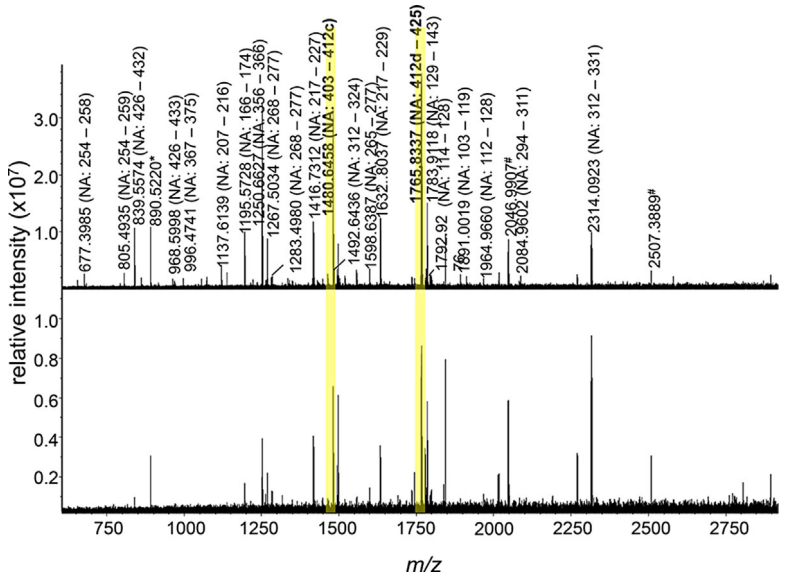

FIGURE 10. MALDI mass spectra of the products of a dual Lys-C/Glu-C digest released from untreated and cyanidin-3-sambubiocide treated neuraminidase. Reprinted from Swaminathan K et al. (2013) with permission [Springer].

Computational molecular docking experiments confirmed these results. Docking of the cyanidin, absent of its disaccharide to minimize the number of degrees of freedom, to the structure of a N1 neuraminidase monomer showed that it binds within the so-called 430-cavity, a region adjacent to the 150-cavity where zanamivir is known to bind (Fig. 11). In both of the two top-ranked, lowest-energy orientations, the hydroxyl group at the 3 position of chromenylium ring is directed out of the pocket so as to be able to accommodate the disaccharide at this position which itself may impede sialic acids from binding in the neighboring 150-cavity. The 430-cavity is a reported secondary sialic acid binding site that has the potential to be exploited for the binding of new inhibitors given it is remote from known resistance mutations.

In accord with the molecular-based studies, the anthocyanin was shown to inhibit influenza neuraminidase in a sialidase inhibition assay. The anthocyanin exhibited an IC_{50} of 72 μM against a type A N1 neuraminidase. Although a significantly poorer inhibitor than the rationally designed zanamivir, it, nonetheless, provides a good starting template from which to design an optimal inhibitor based on the structure of this natural product.

Another class of compounds with similar structural features to anthocyanins were also found to inhibit influenza neuraminidase. Prevalent in the leaves of green tea, cathechins are a class of flavonoids that have recently attracted interest for their potential to inhibit the propagation of influenza and other viruses. Like the anthocyanins, however, their molecular basis of their mode of action was largely unknown. The binding of three catechins, known as epigallocatechin gallate (EGCG), epicatechin gallate (ECG), and catechin-5-gallate (C5G), was recently investigated by MALDI mass spectrometry in

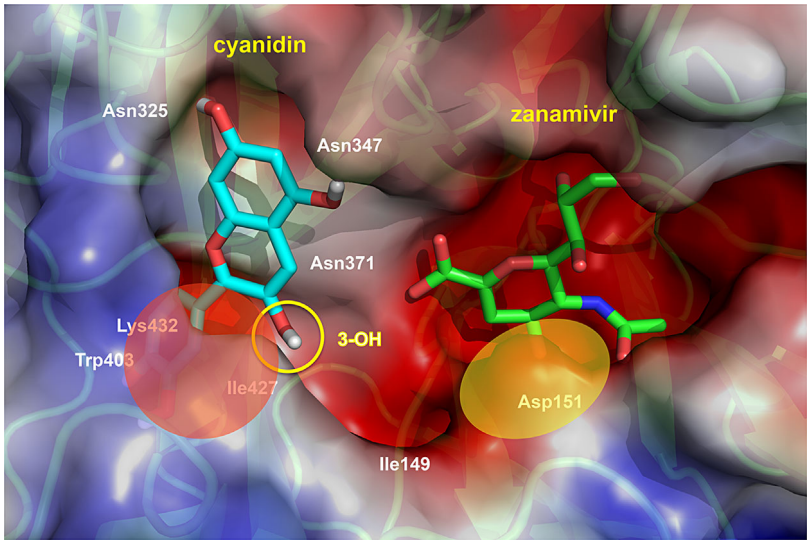

FIGURE 11. Structure of a N1 neuraminidase monomer (PDB ID: 3NSS) in the region of the 430 and 150-cavities showing the location of bound cyanidin and zanamivir. Reprinted from Swaminathan K et al. (2013) with permission [Springer].

conjunction with companion inhibition assays and computational molecular docking (Müller & Downard, 2015). An *in vivo* neuraminidase inhibition assay, followed by confocal microscopy, found that all three catechins resulted in a dose-dependent reduction in neuraminidase activity where complete inhibition was observed at an inhibitor concentration of 100 μM.

The molecular basis of this inhibition was examined by the MALDI-MS approach and found to be similar to that of the cyanidin. The MALDI mass spectra of untreated and catechin-treated neuraminidase revealed all three catechins bound in the vicinity of NA residues 426–433 (Müller & Downard, 2015). Catechin EGCG bound to an additional peptide segment in close proximity comprising NA residues 412–425. Like the anthocyanins, the catechins were also found to bind in the vicinity of residue 430, a result not unexpected given their similar structures (see Fig. 9). Molecular docking revealed both ECGC and ECG adopt a similar orientation with their chromenylium ring located within the 430 cavity with their galloyl group at the 3-position directed toward residue Asp 151. With further structural refinement, their inhibitory properties could be optimized for the development of a new antiviral treatment against circulating strains of the influenza virus.

B. Inhibitor to Influenza Hemagglutinin

Although inhibitors to neuraminidase constitute those currently prescribed, there are advantages in the development and application of therapeutics that target the surface hemagglutinin. This glycoprotein binds to host cell surface receptors to facilitate virus entry. Inhibiting this initial step, versus the latter release of progeny viruses from host cells after replication has already taken place, make it an ideal target of an antiviral agent.

Arbidol is a broad-spectrum antiviral that has been used in the treatment of various respiratory infections including influenza. Within an hour of the pretreatment of infected cells with arbidol, yields of both type A and B influenza virus were reduced by 70–80% (Boriskin et al., 2008). Approved for use in China and Russia, it is believed to arbidol inhibits virus-mediated fusion to block viral entry into the host cell (Boriskin et al., 2008).

To molecular basis of the mode of action of arbidol was investigated using the indirect mass spectrometry approach (Nasser et al., 2013). Recombinant hemagglutinin was incubated with an excess of arbidol, the protein–inhibitor complex was run on a native polyacrylamide gel aside a sample of the untreated protein and, after its blind excision, the untreated and arbidol-treated hemagglutinin were digested in-gel with endoproteinase Glu-C.

The MALDI mass spectra recorded for each sample are shown in Figure 12. The spectra are very similar in appearance with the exception of a marked decrease in the relative abundance of the peptide ions at *m/z* 2109 (highlighted) associated with residues 448–464 of the full-length protein, or residues 104–120 of the HA2 subunit. The relative peak areas of all HA ions were compared, in replicate experiments and with the assistance of the PRISM algorithm (Ho, Morrissey, & Downard, 2007), and found to decrease by 11.8% (absolute) only for this peptide segment. All other peptide ions did not change in relative area by more than 5.5%. Support for the binding of arbidol to a region of the HA2 subunit comes from the separate chymotryptic digest (data not shown). In this case, ions at *m/z* 1367.6244 corresponding to HA0 residues 453–463 (or HA2 residues 109–119) also undergo the largest change in relative area when spectra of the untreated and treated protein are considered. However, in this case, the small relative area of the peak in the untreated hemagglutinin spectrum did not alone allow for a confident prediction of binding.

Companion molecular docking calculations were in accord with the results of the MS assay. The highest ranked, lowest energy, poses were those in which arbidol was bound to the HA2 subunit, in two different orientations at approximately 180° to one another, in the vicinity of residues 118–123 (Fig. 13). Both

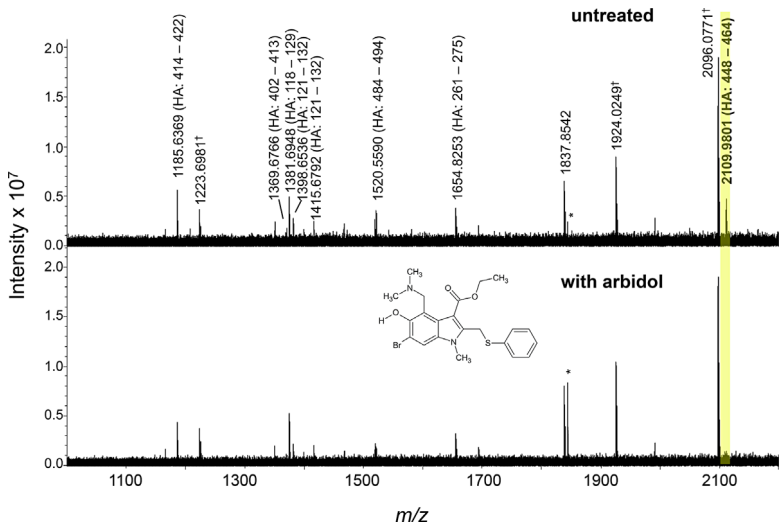

FIGURE 12. MALDI mass spectra recorded of an in-gel endoproteinase Glu-C digested influenza hemagglutinin before and after treatment with arbidol. Reprinted from Nasser Z et al. (2013) with permission [Elsevier].

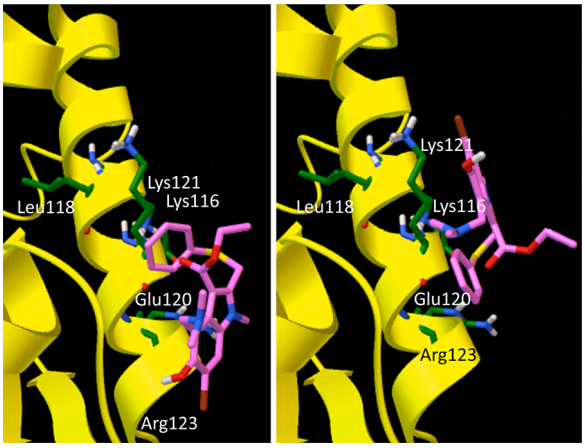

FIGURE 13. Structure of the HA2 subunit of influenza hemagglutinin (PDB ID: 3LZG) showing the location of bound arbidol in the two top ranked poses. Reprinted from Nasser Z et al. (2013) with permission [Elsevier].

the mass spectrometry and molecular docking results support a known arbidol resistance mutation K116R (or residue 117 in structure 3LZG) that residues within this peptide segment (Leneva et al., 2009).

IX. SENSITIVITY OF APPROACH TO DETECT THE RELATIVE AFFINITY OF PROTEIN–INHIBITOR INTERACTIONS

Based on promising results across the range of applications described above, a study was undertaken to investigate the sensitivity of the mass spectrometry based approach in the context of an investigation of the inhibitory potential of structurally related compounds. The ability of the approach to identify the relative affinity of these antiviral inhibitors to their target protein was examined.

Two compounds that are structurally similar to the anthocyanin cyanidin-3-sambubiocide are pelargonidin and delphinidin. Both feature a chromenylium ring supporting three hydroxyl groups at positions 3, 5, and 7 but differ in the number of hydroxyl substituents attached to the phenyl ring. As it is this phenyl ring that is buried within the 430-cavity, shown above to be critical to their function, these substituents were expected to impact upon the interaction of the inhibitors with influenza neuraminidase.

Pelargonidin contains a single hydroxyl group at the 4′ position, while delphinidin contains three hydroxyl groups, one more than the cyanidin, at the 3′, 4′, and 5′ positions. All three compounds were studied in their aglycone anthocyanidin-form, without the 3-hydroxyl group attached to the chromenylium ring.

MALDI mass spectra were obtained from the sequential endoproteinase Lys-C and Glu-C digestion of untreated influenza neuraminidase and that treated separately with pelargonidin and delphinidin. The mean relative peak areas for the neuraminidase peptide ions comprising residues 403–412c and 412d–425 decreased by 12.5 and 20.6% in the presence of pelargonidin and 12.6 and 33.2% in the presence of delphinidin. In the case of this latter compound, an additional peptide segment comprising NA residues 356–366 is also found to bind based on a decrease in the relative peak area of 12.30%. All remaining peptide areas differed in relative area by 10% (absolute) or less.

As part of the same study, the half-maximum inhibitory concentrations (IC_{50}) for each anthocyanidin were measured. These values of 74.87 μM for the cyanidin, 91.54 μM for pelargonidin, and 64.41 μM for delphinidin were plotted relative to the summed total area decrease of all peptide segments that found to bind each inhibitor (Fig. 14). Despite the very different nature of the experiments and datasets, the plot reveals a near linear relationship that demonstrated the reliability of the MALDI-MS results in the context of the inhibition assays. This same close correlation was also observed when the MS results from the binding of zanamivir and DANA to influenza neuraminidase (Swaminathan & Downard, 2012) were compared with their measured inhibitory concentrations.

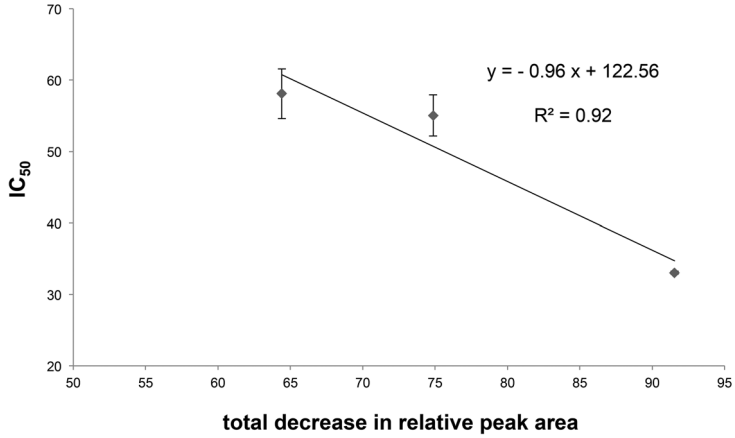

FIGURE 14. Plot of half maximum inhibitory concentrations (IC50) for cyanidin, pelargonidin, and delphinidin versus the summed total relative area decrease of peptide segments found to bind each inhibitor by MALDI-MS. Reprinted from Swaminathan K, Müller P, Downard KM. (2013) with permission [Elsevier].

X. CONCLUSIONS

The ability of the indirect MALDI mass spectrometry approach, later described as "intensity-fading," to both detect and investigate the nature of protein and other macromolecular interactions has wide applicability. Despite preconceived notions that specific non-covalent interactions should not survive on a MALDI sample surface, or during analysis and detection, the examples presented in this review demonstrate otherwise. Moreover, where studied, a good correlation has been found between the mass spectrometry results and other biochemical assays and approaches used to independently confirm such interactions. While the lowest association constant at which complexes can be detected and studied by the indirect MALDI-MS method remains unknown, its successful application across a range of protein systems suggest it has broad potential. Although some care needs to be exercised in the implementation of control experiments, and the need to differentiate specific from nonspecific interactions is ever present, the value and potential of this indirect MALDI approach has been largely overlooked and underestimated. Importantly, it has been shown to be compatible with gel-based separation techniques that allow it to be implemented as part of a functional proteomics strategy.

ACKNOWLEDGMENTS

The research reviewed in this article was supported with funds from the Australian Research Council in the form of Discovery Project Grants (DP0449800, DP0770619, and DP140100591) to the author.

REFERENCES

Axelsson J, Hoberg A-M, Waterson C, Myatt P, Shield GI, Varney J, Haddleton DM, Derrick PJ. 1997. Improved reproducibility and increased signal intensity in matrix-assisted laser desorption/ionization as a result of electrospray sample preparation. Rapid Commun Mass Spectrom 11:209–213.

Bolbach G. 2005. Matrix-assisted laser desorption/ionization analysis of non-covalent complexes: Fundamentals and applications. Curr Pharm Des 11:2535–2557.

Boriskin YS, Leneva IA, Pécheur EI, Polyak SJ. 2008. Arbidol: A broad-spectrum antiviral compound that blocks viral fusion. Curr Med Chem 15:997–1005.

Breuker K, Knochenmuss R, Zhang J, Stortelder A, Zenobi R. 2003. Thermodynamic control of final ion distributions in MALDI: In-plume proton transfer reactions. Int J Mass Spectrom 216:211–222.

Brown RS, Lennon JJ. 1995. Mass resolution improvement by incorporation of pulsed ion extraction in a matrix-assisted laser desorption/ionization linear time-of-flight mass spectrometer. Anal Chem 67:1998–2003.

Cohen LRH, Strupat K, Hillenkamp F. 1997. Analysis of quaternary protein ensembles by matrix assisted laser desorption/ionization mass spectrometry. J Am Soc Mass Spectrom 8:1046–1052.

Colby SM, King TB, Reilly JP. 1994. Improving the resolution of matrix-assisted laser desorption/ionization time-of-flight mass spectrometry by exploiting the correlation between ion position and velocity. Rapid Commun Mass Spectrom 8:865–868.

Downard KM. 2006. Ions of the interactome—The role of mass spectrometry in the study of protein interactions in proteomics and structural biology. Proteomics 6:5374–5384.

Downard KM. 2007. Softly, softly—Detection of protein complexes by matrix-assisted Laser desorption ionization mass spectrometry, in *Mass Spectrometry of Protein Interactions*. New York: Wiley. pp. 25–43.

Downard KM. 2013. An immunoproteomics approach to screen the antigenicity of the influenza virus. In: Twine S, Fulton K, editors. Methods in molecular biology: Immunoproteomics. New Jersey USA: Humana Press. pp. 141–153.

Downard KM, Morrissey B. 2007. Fingerprinting a killer: Surveillance of the influenza virus by mass spectrometry. Analyst 132:611–614.

Dreisewerd K, Schuerenberg M, Karas M, Hillenkamp F. 1995. Influence of the laser intensity and spot size on the desorption of molecules and ions in matrix-assisted laser desorption/ionization with a uniform beam profile. Intl J Mass Spectrom Ion Proc 141:127–148.

Dreisewerd K. 2003. The desorption process in MALDI. Chem Rev 13:395–426.

Ehring H, Karas M, Hillenkamp F. 1992. Role of photoionization and photochemistry in ionization processes of organic molecules and relevance for matrix-assisted laser desorption lonization mass spectrometry. Org Mass Spectrom 27:472–480.

Erijman A, Rosenthal E, Shifman JM. 2014. How structure defines affinity in protein-protein interactions. PLoS ONE 9:e110085.

Farmer TB, Caprioli RM. 1998. Determination of protein-protein interactions by matrix-assisted laser desorption/ionization mass spectrometry. J Mass Spectrom 33:697–704.

Fenn JB. 2003. Electrospray wings for molecular elephants (Nobel lecture). Angew Chem Int Ed 42:3871–3894.

Fenn JB, Mann M, Meng CK, Wong SF, Whitehouse CM. 1989. Electrospray ionization for mass spectrometry of large biomolecules. Science 246:64–71.

Fontana A, de Laureto PP, Spolaore B, Frare E, Picotti P, Zambonin M. 2004. Probing protein structure by limited proteolysis. Acta Biochim Pol 51:299–321.

Frankevich V, Zhang J, Friess SD, Dashtiev M, Zenobi R. 2003. Role of electrons in laser desorption/ionization mass spectrometry. Anal Chem 22:6063–6067.

Ganem B, Li YT, Henion JD. 1991a. Detection of noncovalent receptor-ligand complexes by mass spectrometry. J Am Chem Soc 113: 6294–6296.

Ganem B, Li YT, Henion JD. 1991b. Observation of noncovalent enzyme-substrate and enzyme-product complexes by ion-spray mass spectrometry. J Am Chem Soc 113:7818–7819.

Ho JWK, Morrissey B, Downard KM. 2007. A computer program for the identification of protein interactions from the spectra of masses (PRISM). J Am Soc Mass Spectrom 18:563–566.

Hutchens TW, Yip TT. 1993. New desorption strategies for the mass spectrometric analysis of macromolecule. Rapid Commun Mass Spectrom 7:576–580.

Karas M, Hillenkamp F. 1988. Laser desorption ionization of proteins with molecular masses exceeding 10000 daltons. Anal Chem 60:2299–2301.

Karas M, Krüger R. 2003. Ion formation in MALDI: The cluster ionization mechanism. Chem Rev 103:427–440.

Katz JM, Hancock K, Xu X. 2011. Serologic assays for influenza surveillance, diagnosis and vaccine evaluation. Expert Rev Anti Infect Ther 9:669–683.

Kiselar JG, Downard KM. 1999a. Direct identification of protein epitopes by mass spectrometry without immobilization of antibody and isolation of antibody-peptide complexes. Anal Chem 17:1792–1801.

Kiselar JG, Downard KM. 1999b. Antigenic surveillance of the influenza virus by mass spectrometry. Biochemistry 43:14185–14191.

Kiselar JG, Downard KM. 2000. Preservation and detection of specific antibody-peptide complexes by matrix-assisted laser desorption ionization mass spectrometry. J Am Soc Mass Spectrom 11:746–750.

Konermann L, Pan J, Liu YH. 2011. Hydrogen exchange mass spectrometry for studying protein structure and dynamics. Chem Soc Rev 40: 1224–1234.

Knochenmuss R. 2002. A quantitative model of ultraviolet matrix-assisted laser desorption/ionization. J Mass Spectrom 37:867–877.

Knochenmuss R, Zenobi R. 2003. MALDI ionization: The role of in-plume processes. Chem Rev 13:441–452.

Kratzer R, Eckerskorn C, Karas M, Lottspeich F. 1998. Suppression effects in enzymatic peptide ladder sequencing using ultraviolet—matrix assisted laser desorption/ionization—mass spectrometry. Electrophoresis 19:1910–1919.

Law KP, Larkin JR. 2011. Recent advances in SALDI-MS techniques and their chemical and bioanalytical applications. Anal Bioanal Chem 399:597–622.

Leneva IA, Russell RJ, Boriskin YS, Hay AJ. 2009. Characteristics of arbidol-resistant mutants of influenza virus: Implications for the mechanism of anti-influenza action of arbidol. Antiviral Res 81:132–140.

Ma L, Wang Z, Liu S, Song F, Liu Z, Liu S. 2013. Screening calmodulin-binding ligands using intensity-fading matrix-assisted laser desorption/ionization mass spectrometry. Rapid Commun Mass Spectrom 27: 1527–1534.

Mackun K, Downard KM. 2003. Strategy for identifying protein-protein Interactions of gel-separated proteins and complexes by mass spectrometry. Anal Biochem 318:60–70.

Mädler S, Erba EB, Zenobi R. 2013. MALDI-ToF mass spectrometry for studying noncovalent complexes of biomolecules. Top Curr Chem 331:1–36.

Maleknia SD, Downard KM. 2014. Advances in radical probe mass spectrometry for protein footprinting in chemical biology applications. Chem Soc Rev 43:3244–3258.

Mamyrin B. 2001. Time-of-flight mass spectrometry (concepts, achievements, and prospects). Int J Mass Spectrom 206:251–266.

Mendoza VL, Vachet RW. 2009. Probing protein structure by amino acid-specific covalent labeling and mass spectrometry. Mass Spectrom Rev 28:785–815.

Mock KK, Sutton CW, Cottrell JS. 1992. Sample immobilization protocols for matrix-assisted laser-desorption mass spectrometry. Rapid Commun Mass Spectrom 6:233–238.

Moniatte M, Lesieur C, Vecsy-Semjen B, Buckley JT, Pattus F, van der Goot FG, Van Dorsselaer A. 1997. Matrix-assisted laser desorption-ionization time-of-flight mass spectrometry in the subunit stoichiometry of high mass non-covalent complexes. Int J Mass Spectrom 169/170: 179–199.

Morrissey B, Downard KM. 2006. A proteomics approach to survey the antigenicity of the influenza virus by mass spectrometry. Proteomics 6:2034–2041.

Morrissey B, Streamer M, Downard KM. 2007. Antigenic characterisation of H3N2 subtypes of the influenza virus by mass spectrometry. J Virol Methods 145:106–114.

Morrissey B, Downard KM. 2008. Kinetics of antigen-antibody employing a MALDI mass spectrometry immunoassay. Anal Chem 80:7720–7726.

Müller P, Downard KM. 2015. Catechins inhibit influenza neuraminidase and its molecular basis by mass spectrometry. J Pharmaceut Biomed Anal 111:222–230.

Nasser Z, Swaminathan K, Müller P, Downard KM. 2013. In-vitro inhibition of the influenza virus with the anti-viral inhibitor arbidol by a proteomics based approach with mass spectrometry. Antiviral Res 100:399–406.

Nedelkov D, Nelson RW. 2003. Delineating protein-protein interactions via biomolecular interaction analysis-mass spectrometry. J Mol Recogn 16:9–14.

Nelson RW, Krone JR, Bieber AL, Williams P. 1995. Mass-spectrometric immunoassay. Anal Chem 67:1153–1158.

Rosinke B, Strupat K, Hillenkamp F, Rosenbusch J, Dencher N, Krüger U, Galla HJ. 1995. Matrix-assisted laser desorption/ionization mass spectrometry (MALDI-MS) of membrane proteins and non-covalent complexes. J Mass Spectrom 30:1462–1468.

Satoh T, Sato T, Tamura J. 2007. Development of a high-performance MALDI-TOF mass spectrometer utilizing a spiral ion trajectory. J Am Soc Mass Spectrom 18:1318–1323.

Schwahn AB, Downard KM. 2009. Antigenicity of a type A influenza virus through a comparison of hemagglutination inhibition and mass spectrometry immunoassays. J Immunoassay Immunochem 30: 245–261.

Shigeri Y, Inazumi S, Hagihara Y, Yasuda A, Kawasaki H, Arakawa R, Nakata M. 2012. Desorption/ionization efficiency of peptides containing disulfide bonds in matrix-assisted laser desorption/ionization mass spectrometry. Anal Sci 28:295–299.

Swaminathan K, Downard KM. 2012. Anti-viral inhibitor binding to influenza neuraminidase by MALDI mass spectrometry. Anal Chem 84:3725–3730.

Swaminathan K, Dyason JC, Maggioni A, von Itzstein M, Downard KM. 2013. Binding of a natural anthocyanin inhibitor to influenza neuraminidase by mass spectrometry. Anal Bio Chem 405:6563–6572.

Swaminathan K, Müller P, Downard KM. 2014. Substituent effects on the binding of natural product anthocyanidin inhibitors to influenza neuraminidase with mass spectrometry. Anal Chim Acta 828:61–69.

Tang X, Callahan JH, Zhou P, Vertes A. 1995. Non-covalent protein-oligonucleotides interactions monitored by matrix-assisted laser desorption/ionization mass spectrometry. Anal Chem 67: 4542–4548.

Tang N, Tornatore P, Weinberger SR. 2004. Current developments in SELDI affinity technology. Mass Spectrom Rev 23:34–44.

Vavricka CJ, Liu Y, Kiyota H, Sriwilaijaroen N, Qi J, Tanaka K, Wu Y, Li Q, Li Y, Yan J, Suzuki Y, Gao GF. 2013. Influenza neuraminidase operates via a nucleophilic mechanism and can be targeted by covalent inhibitors. Nat Commun 4:1491–1498.

Villanueva J, Yanes O, Querol E, Serrano L, Aviles FX. 2003. Identification of protein ligands in complex biological samples using intensity-fading MALDI-TOF mass spectrometry. Anal Chem 75:3385–3395.

Wang BH, Dreisewerd K, Bahr U, Karas M, Hillenkamp F. 1993. Gas-phase cationization and protonation of neutrals generated by matrix-assisted laser desorption. J Am Soc Mass Spectrom 4:393–398.

Woods AS, Buchsbaum JC, Worrall TA, Berg JM, Cotter RJ. 1995. Matrix-assisted laser desorption ionization of non-covalently bound compounds. Anal Chem 67:4462–4465.

Yanes O, Aviles FX, Roepstorff P, Jørgensen TJ. 2007. Exploring the "intensity fading" phenomenon in the study of noncovalent interactions by MALDI-TOF mass spectrometry. J Am Soc Mass Spectrom 18:359–367.